Continuous Laser Beam Based Optical Detection of Ingredients in Highly Scattering Media

L. Gurdev, **T. Dreischuh**, **O. Vankov**, **E. Toncheva**,
L. Avramov, **D. Stoyanov**

Institute of Electronics, Bulgarian Academy of Sciences,
Sofia 1784, Bulgaria

Abstract. Some preliminary experiments have been performed concerning the possibility of single-sided optical detection of characteristic inhomogeneities (ingredients, e.g., ill places in tissues) hidden in highly-scattering homogeneous host media (e.g., healthy tissues) irradiated by a collimated cw laser beam. The detection is based on comparative analysis of the backscattered-light intensity distributions over the entrance /exit plane of the medium obtained in the presence and absence of ingredients. The obtained experimental results show that inhomogeneities whose contrast exceeds the measurement signal-to-noise ratio can be distinguished at depths of the order of several transport mean free paths of the photon in the scattering medium. The transversal (with respect to the sensing beam) distinguishability distance turns out to be of the same order. The results of the work are physically viewable and interpretable, but a more rigorous substantiation of them is desirable based on appropriate theoretical models.

PACS codes: 42.62.Be, 87.50.W, 87.14.Cc, 87.64.Cc

1 Introduction

The optical-beam-assisted detection and characterization of backward reflecting or scattering objects hidden in highly scattering media is a task of primary importance in the investigations of various turbid media such as, e.g., clouds of space dust, low-visibility (hazy or cloudy) atmosphere, different kinds of tissues, etc. The single-sided (remote and contactless) optical sensing and diagnostics of such media is in fact a type of optical tomography that can be realized using, e.g., interferometric low-coherence light irradiation methods [1], time-to-range resolved pulsed-irradiation methods [2], or stationary continuous-wave (cw) laser beam irradiation methods [3]. The latter type of methods have undergone relatively weaker development so far, but they may have some advantages consisting in avoiding the necessity of using high-repetition-rate short-pulse laser transmitters and fast signal-recording electronics

L. Gurdev, T. Dreischuh, O. Vankov, E. Toncheva, L. Avramov, D. Stoyanov

or sophisticated delicately-adjustable interferometric instruments [1, 2]. A common question of basic significance for all the (single-sided) optical tomography approaches concerns the maximum-achievable depth of clear-cut imaging in the scattering medium. On the basis of different theoretical estimates and experimental investigations it is expected that the limiting depth is of the order of several (say $4 - 6$) transport mean free paths of the photon in the medium [4, 5]. So, the main purpose of the investigations performed in this work is to estimate experimentally the possibilities of detecting and evaluating the disposition and size of contrasting ingredients in highly-scattering media (e.g., ill places in tissues) by means of a scattering-widened cw laser beam, as well as to outline the depth of distinct imaging.

2 Experimental Setup, Method and Materials

The experimental setup employed in this work is similar to that described in Ref. [6]. It is represented schematically in Figure 1 and is intended for measuring the intensity distribution, over a "frontal" (entrance/exit) plane, of the backscattered light from a highly-scattering medium irradiated by a stationary cw laser beam. The beam is incident normally to the frontal plane, and the measurements are performed when the medium (say healthy tissue) contains or not characteristic inhomogeneities (inclusions, ill places). The difference between the images (intensity distributions) with and without inhomogeneities should provide an image of the inhomogeneities themselves. The central unit of the setup is a plexiglass parallelepiped-form container of sizes $12 \times 12 \times 22\,\mathrm{cm}$ that is filled with tissue - mimicking liquid turbid media (phantoms). A laser diode is employed as a source of a nearly collimated cw optical beam of about $20\,\mathrm{mW}$ power, $1.5\,\mathrm{mm}$ radius and wavelength $\lambda = 847\,\mathrm{nm}$. The beam is incident normally on a frontal wall of the container (Figure 1). The axis of the beam inside the container coincides with axis $0z$ whose initial point $0\{0, 0, 0\}$ is lying on the internal frontal wall. Two more axes, $0x$ (hor-
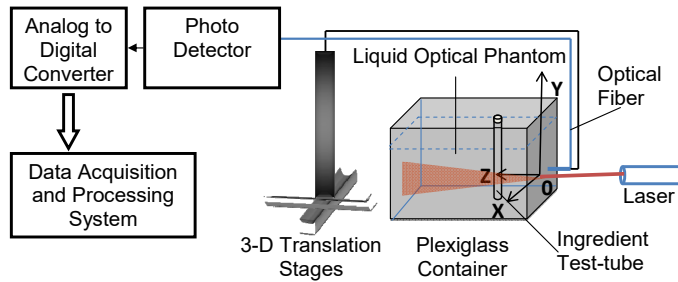

Figure 1: Experimental setup.

izontal) and $0y$ (vertical), lying on the same wall, form along with $0z$ a right coordinate system represented in Figure 1.

The liquid turbid media (phantoms) of interest in this work are dilutions in distilled water of different concentrations of Intralipid 20% (Fresenius Kabi AB, Sweden). Intralipid is a fat emulsion, made up of soybean oil, egg yolk phospholipids, glycerin, and water. These emulsions are widely used in optical experiments to simulate the scattering properties of biological tissues [7, 8]. The main reason for that is the low absorption coefficient at visible and near-infrared wavelengths and the possibility to adjust the scattering coefficient by changing the concentration of the solutions. The Intralipid concentration is considered as the volume fraction of soybean oil and egg lecithin forming the scattering submicron capsules in the dilution [8]. This volume fraction is 22.74% in stock Intralipid-20%.

The inhomogeities used in the experiments are made of the same material as the basic host medium. Certainly, they have a different turbidity, that is, a different concentration of scatterers. The inhomogeneity-mimicking media are introduced into the host medium via test tubes of glass of different diameters perpendicular to the plane $\{0xz\}$. The tubes can be translated in depth and laterally, that is, parallelly to axes $0z$ and $0x$, respectively. The quantity measured in the experiments is the backscattered light power distribution $J(\vec{\rho})$ ($\vec{\rho} = \{x, y\}$) over the external frontal (entry/exit) wall $z = 0$ of the container (with and without inhomogeneities) by using a scanning optical fiber of $0.1\,\mathrm{mm}$ core diameter with an additional accessory to narrow the field of view. The half angle of acceptance of the receiver in this case is estimated to be $\sim 0.01\,\mathrm{rad}$. The receiver aperture radius is about $0.45\,\mathrm{mm}$. The fiber is oriented parallel to the beam axis and is connected with an optical radiometer Rk-5100 (Laser Precision Corp., USA) in external locking regime, with a RqP-546 silicon probe, 14 bits analog-to-digital converter (ADC) and a computer for appropriate data processing. The noise equivalent power (NEP) of the radiometer is $2 \times 10^{-12}\,\mathrm{W}$. Its averaging (low-pass filtering) time constant is chosen to be 1 s. The transversal distribution of the detected power $J(\vec{\rho})$ is measured in fact by scanning the fiber along a horizontal line parallel to axis $0x$ and at some distance ($y = y_{\mathrm{c}} = const$) from it. The fiber scanning is implemented by using a linear translation stage with an integrated stepper motor and controller LTS 300/M (Thorlabs, Inc., USA) ensuring a minimum sampling step of $4\,\mu\mathrm{m}$.

The distribution $J(\vec{\rho})$ represents in fact the intensity distribution of the backscattered light because the receiver aperture radius E and angle of acceptance γ are much smaller respectively than the transversal and angular variation scales of the backscattered light radiance over plane $z = 0$. At known distributions $J(x, y_{\mathrm{c}}) = J_1(x, y_{\mathrm{c}})$ of the medium with in-

homogeneities, and $J(x, y_c) = J_2(x, y_c)$ of the host medium alone, their difference $J_d(x, y_c) = J_1(x, y_c) - J_2(x, y_c)$ should provide an image of the inhomogeneities of interest. Thus, the final quantity to be determined and physically analized is the ingredient (inhomogeneity) signal $J_d(x, y_c)$. The measurement errors of $J_{1,2}(x, y_c)$ may be conditioned by different factors. The experiments are conducted in a dark laboratory at practically entirely removed influence of stray light. NEP of the radiometer is negligible as compared to the least measured power values of interest. Then, the signal fluctuations should mainly be a consequence of the signal-conditioned shot noise [9], the digitizing noise, the laser power fluctuations, and the scintillations due to the random walk of the particles within the scattering volume. In the experiments, a low-pass filtering with $1\,\mathrm{s}$ time constant is conducted along with 400 measurements per point. In this way, the relative root-mean-square (rms) signal fluctuations are reduced to levels of about 1%.

Since J_d is the difference between J_1 and J_2, the error in its determination is, e.g., twice larger than the error in the determination of J_1 or J_2. So, an inhomogeneity would be recognizable in general, if J_d exceeds essentially the summary level of fluctuations of J_1 and J_2. Besides, the inhomogeneity should be disposed at a depth and lateral distance (from the beam axis) not exceeding several transport mean free paths of the photon in the scattering medium in order to avoid an image degradation due to multiple scattering [4, 5, 10].

3 Experimental Results and Discussion

The Intalipid concentrations C_h of the host media employed in the experiments are 0.2%, 0.4% or 0.6%. The corresponding values of the reduced-scattering coefficients μ_{rs} of these media at $\lambda = 847\,\mathrm{nm}$ are about $0.23\,\mathrm{mm}^{-1}$, $0.46\,\mathrm{mm}^{-1}$, and $0.84\,\mathrm{mm}^{-1}$ [10]. The related values of the transport mean free paths of the photon $\mathrm{MFP}_{\mathrm{tr}} = \mu_{\mathrm{rs}}^{-1}$ are respectively about $4.4\,\mathrm{mm}$, $2.2\,\mathrm{mm}$ and $1.2\,\mathrm{mm}$. Note for comparison that the mean value of μ_{rs} of tissues at wavelengths of the same order is accepted to be $\sim 1\,\mathrm{mm}^{-1}$ [11, 12]. According to some estimates obtained in [10], at longer sensing wavelengths within the near-infrared (NIR) spectral range, $\mathrm{MFP}_{\mathrm{tr}}$ is longer, the detected backscattered light power is higher, and the multiple scattering influence is weaker. This means that a deeper clear-cut imaging is achievable in this case, at a lower level of the noise and the multiple scattering background.

Two test tubes are used in the experiments, one of $10\,\mathrm{mm}$ diameter, and another, of $3\,\mathrm{mm}$ diameter. The Intralipid concentrations C_t of the contrasting dilution in the test tubes are chosen so that to obtain inhomogeneity contrast from 20% to 200% at different host-media turbidities.

Clear-cut images of such inhomogeneities are obtainable from depths of the order of several $\mathrm{MFP_{tr}}$ at a relatively low noise level. So one may achieve a clear observation of the image peculiarities. As mentioned above, lower contrast inhomogeneities would be detectable when using longer-wavelength sensing radiation. Increasing the sensing beam power would also increase the measurement signal-to-noise ratio (SNR) and the image detectability and contrast.

The measurements of the backscattered-light intensity distribution are performed with only one or two test tubes disposed in the container with the host medium. In the case of a single tube, it is disposed during the measurements at different depths, and at different lateral positions at a given depth. The intensity distributions are measured first with empty tubes and then with the same tubes filled with the contrasting dilution. The inhomogeneity image is obtained by subtracting the former distribution from the latter one (see also the preceding Section 2).

Below in this Section, we shall consider and discuss various images obtained under different experimental conditions. A set of such images obtained at $C_h = 0.2\%$ with the wider tube filled with $C_t = 0.6\%$ dilution is represented in Figure 2. The inhomogeneity contrast in this case is
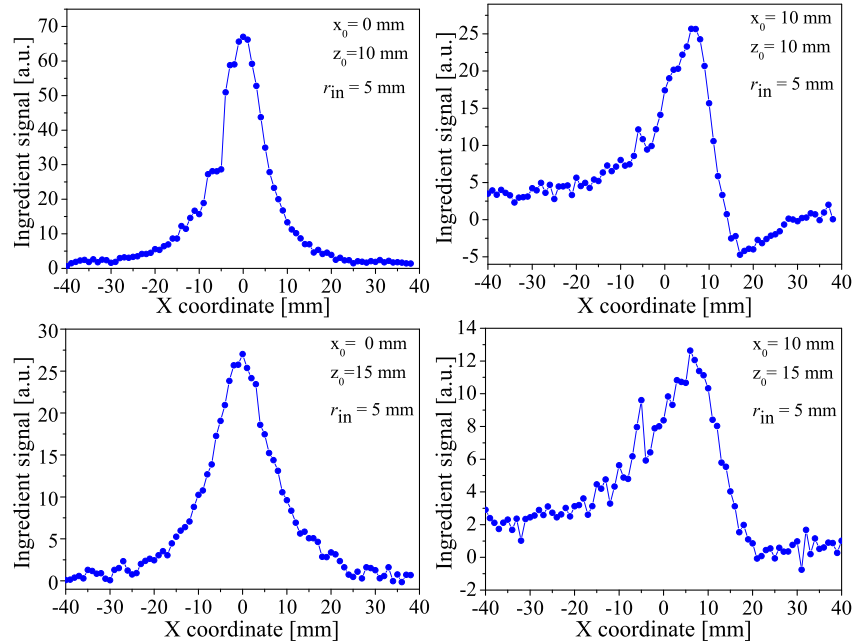

Figure 2: Images of the wider inhomogeneity for different dispositions in the host medium.

$(C_h - C_t)/C_h = 200\%$. The images have been obtained by disposing the tube at depths z_0 of $10\,\mathrm{mm}$ and $15\,\mathrm{mm}$ with respect to the frontal wall of the container. At such depths, the tube is placed first in front of the laser beam and then shifted right successively with a step of $5\,\mathrm{mm}$. The optical receiver is oriented parallel to the laser beam axis (normally to the tube), and is scanned parallelly to axis $0x$, at a distance of $8\,\mathrm{mm}$ from it. It is seen in Figure 2 that the most bright are the images when the tube is set in front of the laser beam. Besides, they are on the average symmetric with respect to the line $0z$, and their half-maximum width is comparable with the width of the inhomogeneity. With increasing the depth the peaks of the images decrease, and they are informative up to a depth of around $20 - 25\,\mathrm{mm}$. At larger depths the image is absorbed by noise. The shift of the tube right from the beam axis leads to an increasing distortion of the images due to their asymmetric disposition with respect to the laser beam. In this case, the left wing of the image is raised up because of a raised detection of multiple-scattered photons in the presence of the inhomogeneity. On the contrary, the reduced number of (scattered) photons right from the inhomogeneity leads to a fall off of the right wing even below zero. Also, the peak of the image is shifted left from the lateral position x_0 of the inhomogeneity because of the stronger scattering from the left side of it. Note that the measurements performed show as well that when an inhomogeneity is positioned left from the laser beam, the distortion of its image is on the average mirror - symmetrical to that of the corresponding right position of it. Also, the images of inhomogeneities disposed at distances x_0 of $5\,\mathrm{mm}$ and $10\,\mathrm{mm}$ from the laser beam are informative to depths z_0 of $15 - 20\,\mathrm{mm}$. At lateral distances of $15\,\mathrm{mm}$ and $20\,\mathrm{mm}$, the images are informative at maximum depths of immersion about $10 - 15\,\mathrm{mm}$.

In Figure 3 we have represented some images of the wider inhomogeneity disposed at a depth of $10\,\mathrm{mm}$ in front of the laser beam. The values of C_h and C_t are respectively 0.2% and 0.3% (50% contrast, Figure 3a), and 0.6%, and 0.82% (37% contrast, Figure 3b). It is seen in the Figure that these relatively low-contrast inhomogeneities (one of them in a host medium with tissue-like turbidity) are clearly detectable at depths of at least $10 - 15\,\mathrm{mm}$.

The experiments with the narrower test tube lead in general to analogous results to those obtained with the wider tube (Figure 4). Some differences consist in that, first, the signal is weaker and the noise is relativery stronger. Second, the shot noise and multiple-scattered photons penetrating the receiver disguise the true size of an inhomogeneity when disposed deeper. Third, the peaks of the images are still sharper than those in the preceding case. As mentioned above, the use of more intensive, longer-wavelength sensing radiation is expected to reduce the effect of the noise and the multiple scattering.
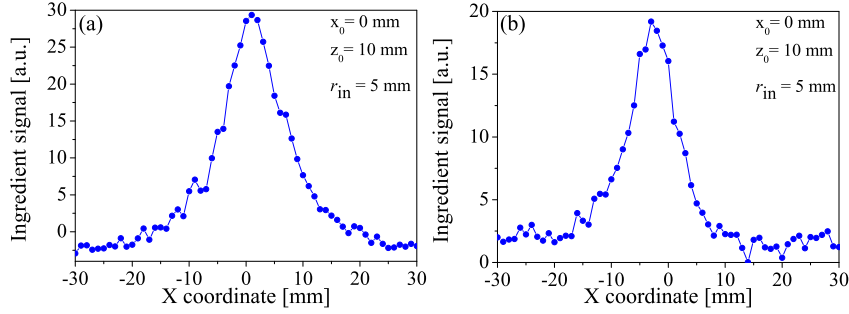
Figure 3: Images of the wider inhomogeneity disposed in front of the laser beam at a depth of $10\,\mathrm{mm}$, in host media of 0.2% (a) and 0.6% (b) Intralipid concentration corresponding to contrast of 50% and 37%.
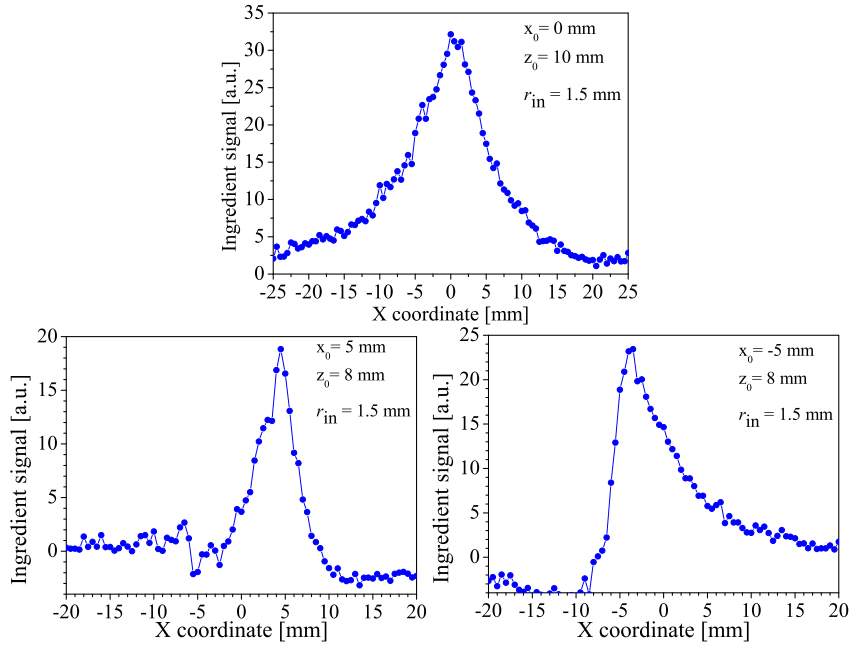

Figure 4: Images of the thinner inhomogeneity of concentration $C_t = 0.6\%$ for different dispositions in a host medium witn $C_h = 0.2\%$.

Experiments have been performed as well with both the tubes placed in the container, both right or left from the laser beam or one of them left and the another right from the laser beam. In the former case (Figures 5a), the images of both the inhomogeneities are more distinguishable when the thinner tube is nearer the laser beam because of a weaker
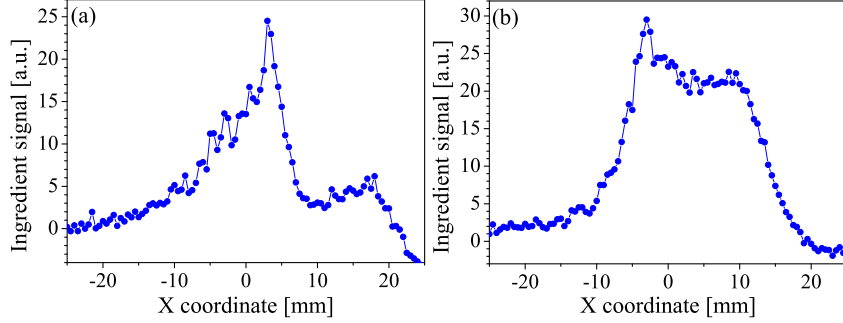
Figure 5: Images of pairs of inhomogeneities of $C_t = 0.8\%$ in a host medium of $C_h = 0.2\%$. (a) The thinner tube is disposed at a depth of 8 mm and a lateral distance of 4 mm while the wider one is disposed at a depth of 11 mm and a lateral distance of 21.7 mm, both right from the laser beam. (b) The thinner tube is disposed left from the laser beam at a depth of 8 mm and a lateral distance of 7 mm while the wider one is disposed rigth from the laser beam at a depth of 11 mm and a lateral distance of 10.7 mm.

influence of the multiple-scattered photons. In the latter case (Figures 5b), the disguising effect of the noise and backscattered photons is stronger, but the images are still distinguishable. As a whole, at equal depths and lateral distances, the peaks of the images of the wider inhomogeneity are higher than those of the thinner one because of stronger backscattered signal. Also, because of stronger attenuation of the light fluxes the peak heights decrease with the increase of the depth and lateral distance of the detected inhomogeneities.

The above-discussed behaviour of the detected images can be roughly described in general by some approximate theory like that employed in Ref. [6]. A more detailed description of some additional peculiarities of this behaviour, such as the image distortions, is possible on the basis of a more rigorous and complicated theoretical apporoach. In experimental plan, the images could be improved by using more intensive and longer-wavelength NIR sensing radiation.

4 Conclusions

The experimental results obtained in the work show that inhomogeneities whose contrast exceeds the measurement signal-to-noise ratio can indeed be distinguished at depths of the order of several (4-6) transport mean free paths of the photon in the scattering medium. The transversal (with respect to the sensing laser beam axis) distinguishabil-

ity distance turns out to be of the same order. In this case, one may estimate the inhomogeneity positions and sizes, but some distortions of the images take plase due to different factors. One of them is certainly the measurement shot noise. Besides, the images of the inclusions disposed aside from the beam axis become asymmetric due probably to asymmetric single and multiple scattering from (through) them with respect to the receiver. The multiple scattering should also be the reason of widening the images that is especially noticeable in the cases of using narrow test tubes. The relative effect of the shot noise can be lowered by increasing the sensing beam power. This in turn would increase the ability of detecting lower-contrast inhomogeneities of interest for the biomedical practice. The multiple scattering influence can be damped for instance by using polarization-sensitive detection of the optical signals. At last, the transport mean free path of the photon in a highly scattering medium can be enlarged by using longer-wavelength sensing radiation. This would allow one to lower the multiple scattering and noise influence and to achieve a deeper clear-cut sensing in media of higher turbidity near that of tissues. An idealized approximate theoretical description of the experiments conducted here and the corresponding expected results provide of course an idealized picture. A more adequate (if achievable) but too complicated theory would be perhaps impracticable. In any case, the results obtained in the work are physically viewable and interpretable, and further thorough experiments and theoretical efforts should make more precise the conclusions deduced here.

Acknowledgments

Bibliography

[1] W. Drexler and J.G. Fujimoto (2008) *Optical Coherence Tomography: Technology and Applications*, Springer, Berlin, Germany.

[2] L. Gurdev, T. Dreischuh, and D. Stoyanov (2007) *Proc. SPIE* **6604** 66042I.

[3] M. Patachia, S. Banita, C. Popa, and D. C. Dumitras (2015) *Rom. Rep. Phys.* **67** 412–422.

[4] K. Bizheva, A. Siegel, and D. Boas (1998) *Phys. Rev. E* **58** 7664–7667.

[5] L. Gurdev, T. Dreischuh, O. Vankov, I. Bliznakova, L. Avramov, and D. Stoyanov (2014) *Appl. Phys. B* **115** 427–441.

[6] L. Gurdev, T. Dreischuh, O. Vankov, I. Bliznakova, L. Avramov, and D. Stoyanov (2016) *Proc. SPIE*, accepted.

[7] R. Michels, F. Foschum, and A. Kienle (2008) *Opt. Express* **16**, 5907–5925.

L. Gurdev, T. Dreischuh, O. Vankov, E. Toncheva, L. Avramov, D. Stoyanov

[8] H.J. van Staveren, C.J. Moes, J. van Marie, S.A. Prahl, and M.J.C. van Gemert (1991) *Appl. Opt.* **30** 4507–4514.

[9] R. M. Measures (1984) *Laser Remote Sensing*, Wiley, New York, USA.

[10] T. Dreischuh, L. Gurdev, O. Vankov, D. Stoyanov and L. Avramov (2015) *J. Phys.: Conf. Ser.* **594** 012030.

[11] A.N. Bashkatov, E.A. Genina, V.I. Kochubey, V.V. Tuchin (2005) *J. Phys. D: Appl. Phys.* **38** 2543–2555.

[12] T.L. Troy, S.N. Thennadil (2001) *J Biomed Opt.* **6** 167–176.